Electronic Supplementary Material (ESI) for Chemical Science.

Supplementary Materials

Large negative differential conductance and its transformation in a single radical molecule

Contents:

1. Tip state

The tip use in the experiment was first poked on clean Au(111) surface and the surface state was seen in the scanning tunneling spectroscopy. No obvious features were found around the zero bias.

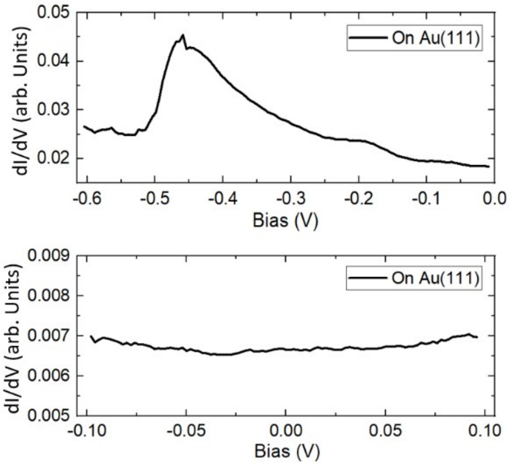

SFigure 1 dI/dV spectra on Au(111). The set point is (-0.6 V, 0.5 nA) for the top spectrum and (-0.1 V, 0.15 nA) for the bottom one.

2. Tunneling junction height at different set points

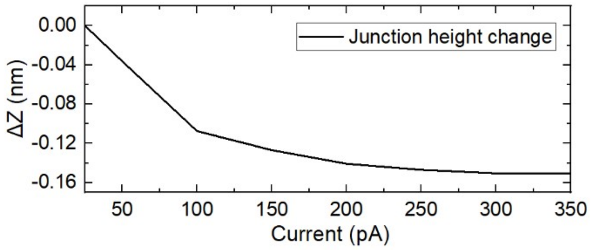

SFigure 2 Junction Height at different set points. The height has been set zero at 25 pA.

3. Peak to valley ratio at different tunneling junction height

The peak to valley ratio for NDC spectra is defined by the $PVR = I_{peak}/I_{valley}$, in which the peak current I_{peak} and the valley current I_{valley} are the amplitude of the current before and after the transition around 45 mV. These values are extracted from the I-V curves as displayed in SFigure 3, for current set point varies from 25 pA to 150 pA. For current set points more than 150 pA, the I-V curves present PDC feature and their PVR values are thus not available.

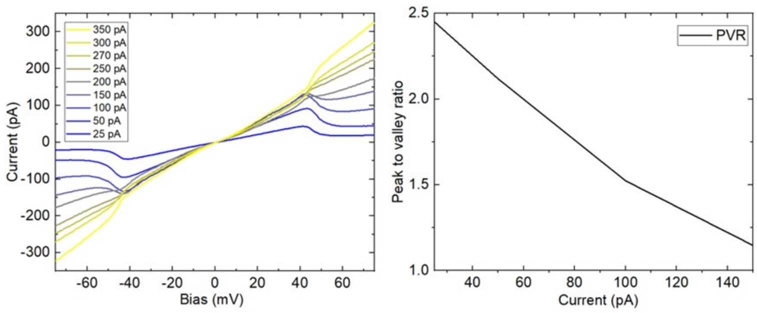

SFigure 3 Left: I-V tunneling spectra at different set point. Right: extracted PVR values from I-V spectra.

4. Phonon modes of the CTPO molecule

Phonon modes calculation and atomic charge analysis of geometry optimized CTPO molecule were completed by ORCA 5.0.4[1]. The geometries of type A and type B molecules are extracted from AIMD. The geometry optimization and frequency calculations were calculated with the Perdew–Burke–Ernzerhof zero-parameter global hybrid functional (PBE0)[2, 3]. The def-TZVP[4] Gaussian AO basis set and def2/J[5] auxiliary basis set were employed. The DFT-D3 correction was used in calculations. The energy convergence threshold was set as 1E-6 Ha. The displacement change threshold was set as 5.3E-4 Å.

Phonon Mode	Type A Excitation Energy(meV)	Type B Excitation Energy(meV)
1	4.08332	12.14456
2	8.7172	15.53596

3	11.72668	17.00288
4	18.27512	22.49112
5	18.90256	24.4156
6	19.50024	26.44424
7	21.8178	34.2984
8	25.23648	37.603
9	27.56148	37.88696
10	28.8548	38.49952
11	35.10936	39.0414
12	37.48024	39.34272
13	38.06924	40.66084
14	39.35512	42.0546
15	41.65656	42.9102
16	46.34624	46.4938
17	48.86344	50.30556
18	54.84272	54.6902
19	56.92964	57.7096
20	66.45036	65.35296
21	68.40832	69.75868
22	70.68372	70.55104
23	75.52716	76.84776
24	76.44352	79.25708
25	82.16488	81.65648
26	87.11372	85.93944
27	94.71988	94.39004
28	96.78944	99.02888

Stable1 Calculated phonon modes of both type A and type B CTPO molecules.

5. Simulation of a cluster of eight CTPO molecules on surface.

Simulations of a cluster of eight CTPO molecules on Au(111) were performed using CP2K software packages[6], based on the GFN-xTB method[7] in the Quickstep module. The structure of single CTPO molecule was first obtained by ORCA simulation. A 29.9818 × 31.735 × 25 Å cell was used to run AIMD calculation. The nearest Au atom distance was set as 2.885 Å (experimental value). A single layer of Au atoms was used as substrate and the Au atoms were fixed in the calculation. The system was simulated with the NVT ensemble and the temperature was controlled with a CSVR thermostat. More than 80 ps time length was used to obtain the molecular structure of CTPO/Au(111). The time step was set as 1 fs. Temperature, potential energy and root means square displacement/deviation (RMSD) trajectories were used to indicate the simulation state of AIMD. The results have been displayed in Sfigure 4. The system was fully balanced after 40 ps.

To simulate the STM images, the DFT simulation was implemented by CP2K. The self-consistent field (SCF) calculation is based the combination of Gaussian and plane-wave hybrid (GPW) methods with PBE functionals[2]. DFT-D3 correction was adopted in the calculation. The truncation of plane wave was 500 Ry. The DZVP-MOLOPT-SR-GTH basis set[8, 9] was cutoff at 52 Ry. The convergence criteria for SCF was set to 1e−8 Ry. The energy correction threshold was set to 1e-12 Ry.

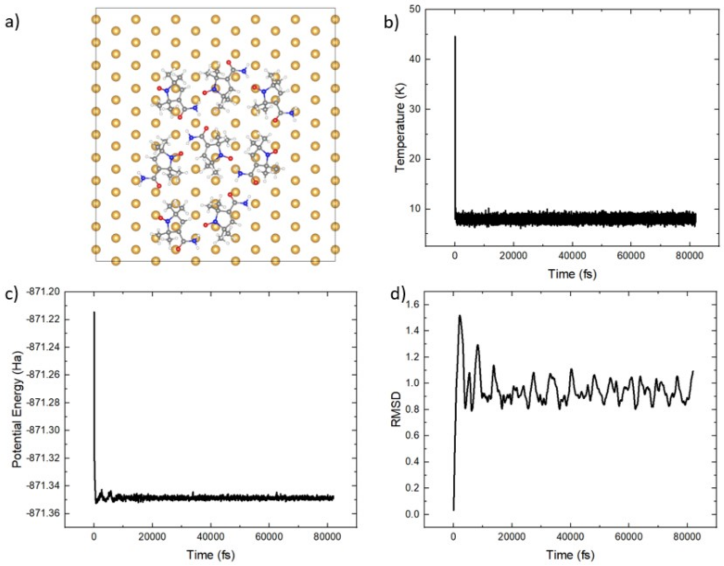

SFigure 4 AIMD simulation results. a) Top view of relaxed CTPO molecules on Au(111). b), c) and d) are trajectories of temperature, potential energy, and RMSD, respectively.

6. Non-covalent interaction analysis

To evaluate the hydrogen bond between type B and type A molecules, non-covalent interaction[10] was simulated by QE software.

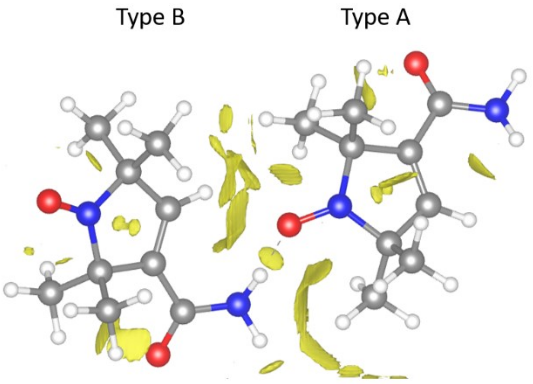

SFigure 5 Hydrogen bond between type B and type A molecule. The isosurface value is set as 0.5.

7. Calculation of single CTPO molecule adsorbed on surface

To obtain molecule adsorption geometry and local density of states of single CTPO molecule adsorpted on Au(111) system, Quantum ESPRESSO software version 6.4.7[11] was employed. The generalized gradient approximation (GGA), Perdew–Burke–Ernzerhof (PBE) exchange–correlation functional[2] and projector-augmented wave (PAW) pseudopotentials[12] were used in the calculation. We used 48 Ry kinetic energy cutoff and 367

Ry density cutoff in calculations which were larger than the recommended values in the pseudopotential files. Spin polarization was not considered. The Brillouin zones were sampled by using the Monkhorst–Pack methodology[13], with Γ point-centered 1 × 1 × 1 grids for relaxation and 3 × 3 × 1 grids for the self-consistent field calculation. A 0.003 Ry width Gaussian smearing was adopted and the self-consistent field calculation convergence threshold was set to 5E-7 Ry in both relaxation calculation and self-consistent field calculation. Force convergence criterion was set as 0.002 Ry/Bohr in relaxation calculation. The semi-empirical Grimme-D3 dispersion correction[14, 15] is applied to describe the long-range van der Waals (vdW) interaction in the systems. We used a 6 × 6 unit cell of Au(111) with four atomic layers in the z-direction, in which the bottom two layers was fixed during the geometry optimization. The vacuum thickness of the slab model was set as 25 Å in the z-direction.

8. Simulation of STM image for a single CTPO molecule

The energy distribution of DOS is used to simulate the STM image. To obtain DOS of the system, non-self-consistent field calculation (NSCF) was executed based on former relaxation and self-consistent field calculation. The Brillouin zones were sampled by using the Monkhorst–Pack methodology, a 12×12×1 grid was used. A 0.001 Ry width Gaussian smearing was adopted and the self-consistent field calculation convergence threshold was set to 1E-8 Ry. Other settings were same as the former calculation.

Calculation indicates that the DOS of radical elements is predominant near the Fermi level, as shown in SFigure 6, thereby enhancing the likelihood of excitation for radical-associated phonon modes compared to other phonon modes. In addition, the results of a single molecule adsorbed on the surface are similar to that for the molecule at the boundary of monolayer (Type B). In other words, the property of type B molecules shall have similar properties as an isolate molecule. Simulated STM image of a single CTPO on Au(111) displays a similar shape in the AIMD simulation, as shown in SFigure 7.

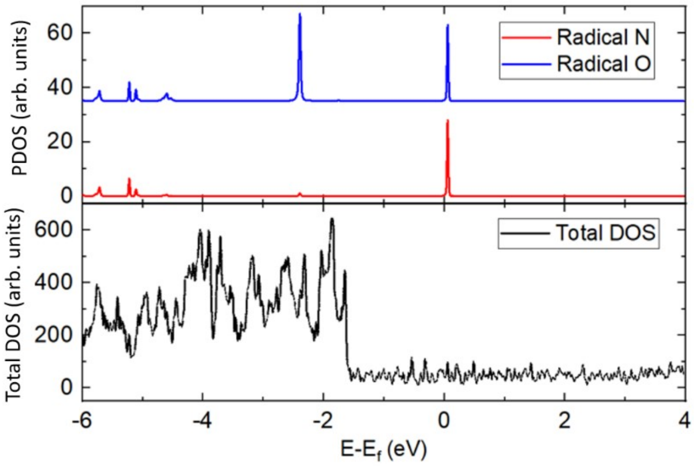

SFigure 6 Projected density of states (PDOS) of N and O on radical group, and the total DOS in the range from -6 eV to 4 eV.

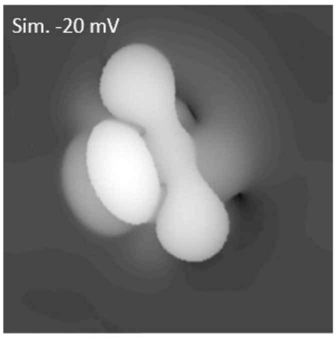

SFigure 7 Simulated STM image of a single CTPO molecule on Au(111).

9. Infrared intensity of CTPO molecule

To evaluate the dipole excitation, infrared (IR) active phonon modes were calculated by ORCA software. The calculation settings were same as those mentioned in Section 4. SFigure 8 shows Infrared activity intensity of all modes between 25 meV and 55 meV, for both type A and type B molecules, as well as a free CTOP molecule. The assigned phonon modes all show noticeable N-O radical related IR intensity.

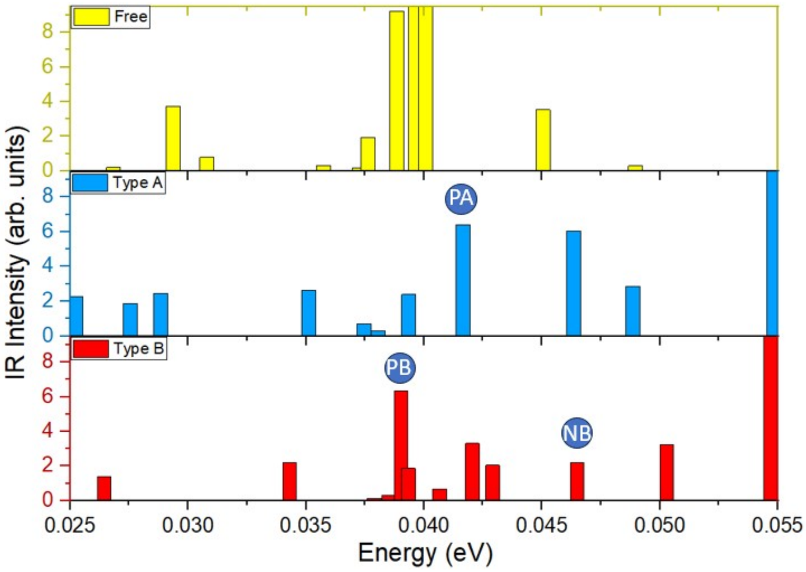

SFigure 8 Infrared activity intensity of the CTPO for each phonon mode.

10. Atomic charge population and dipole moment analysis

Restrained electrostatic potential[16] (RESP) charges were simulated by the combination of CP2K and Multiwfn[17] software. The dipole moment calculation was completed by Multiwfn. The molecule structure was first obtained by AIMD simulation. Then the molecular structure was used to calculate wavefunctions for Multiwfn. The self-consistent field (SCF) calculation is based on the combination of Gaussian and plane-wave hybrid (GPW) methods with PBE functionals. DFT-D3 correction was adopted in the calculation. The TZVP-MOLOPT-SR-GTH basis set was used. The convergence criteria for SCF was set to 5e−8 Ry. The energy correction threshold was set to 1e-12 Ry. Other settings were same as those used when calculating STM images with CP2K software. From SFigure 9c, it is obvious that the RESP charges and magnitude of dipole moments at the left side of molecule is larger than the right side.

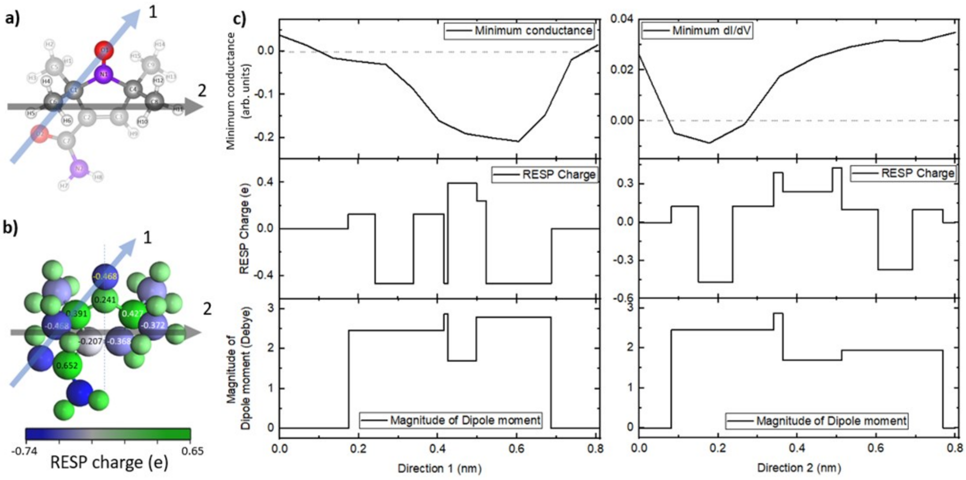

SFigure 9 Atomic charge population and dipole moment analysis. a) molecule structure of type B molecule. The arrows indicate the direction 1 and 2 for IETS spectra measurement in main context. b) RESP charges distribution on type B molecule. The charges are noted on the atoms with different colors. c) Conductance, RESP charges and magnitude of local dipole moment distributions along direction 1 (left) and 2 (right).

11. IETS on type A molecule with different tunneling junction height

We also measured the IETS on type A molecule with different tunneling junction height. The results have been shown in SFigure 10. The PDC position blue shifted by less than 3 meV.

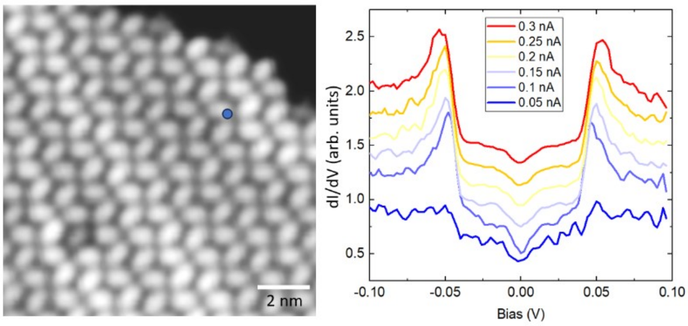

SFigure 10 IETS on type A molecule with different tunneling junction height. Left: topogragh of CTPO monolayer. The set point is (-0.2 V, 20 pA). Right: dI/dV spectra on type A molecule with different set point, from 0.3 nA to 0.05 nA in tunneling current. The curves were offset for clarity. The spectra were acquired at the position marked in the topographic image.

12. Plotting tools

The VESTA[18] and VMD software[19] were used to display the DFT and AIMD results.

References

[1] NEESE F. Software update: The ORCA program system—Version 5.0 [J]. Wiley Interdisciplinary Reviews: Computational Molecular Science, 2022, 12(5): e1606.

[2] PERDEW J P, BURKE K, ERNZERHOF M. Generalized gradient approximation made simple [J]. Physical review letters, 1996, 77(18): 3865.

[3] ADAMO C, BARONE V. Toward reliable density functional methods without adjustable parameters: The PBE0 model [J]. J Chem Phys, 1999, 110(13): 6158-70.

[4] WEIGEND F, AHLRICHS R. Balanced basis sets of split valence, triple zeta valence and quadruple zeta valence quality for H to Rn: Design and assessment of accuracy [J]. Physical Chemistry Chemical Physics, 2005, 7(18): 3297-305.

[5] WEIGEND F. Accurate Coulomb-fitting basis sets for H to Rn [J]. Physical Chemistry Chemical Physics, 2006, 8(9): 1057-65.

[6] KÜHNE T D, IANNUZZI M, DEL BEN M, et al. CP2K: An electronic structure and molecular dynamics software package - Quickstep: Efficient and accurate electronic structure calculations [J]. J Chem Phys, 2020, 152(19): 194103.

[7] GRIMME S, BANNWARTH C, SHUSHKOV P. A Robust and Accurate Tight-Binding Quantum Chemical Method for Structures, Vibrational Frequencies, and Noncovalent Interactions of Large Molecular Systems Parametrized for All spd-Block Elements (=1-86) [J]. J Chem Theory Comput, 2017, 13(5): 1989-2009.

[8] GOEDECKER S, TETER M, HUTTER J. Separable dual-space Gaussian pseudopotentials [J]. Physical Review B, 1996, 54(3): 1703-10.

[9] HARTWIGSEN C, GOEDECKER S, HUTTER J. Relativistic separable dual-space Gaussian pseudopotentials from H to Rn [J]. Physical Review B, 1998, 58(7): 3641-62.

[10] CONTRERAS-GARCÍA J, JOHNSON E R, KEINAN S, et al. NCIPLOT: A Program for Plotting Noncovalent Interaction Regions [J]. J Chem Theory Comput, 2011, 7(3): 625-32.

[11] GIANNOZZI P, ANDREUSSI O, BRUMME T, et al. Advanced capabilities for materials modelling with Quantum ESPRESSO [J]. Journal of physics: Condensed matter, 2017, 29(46): 465901.

[12] DAL CORSO A. Pseudopotentials periodic table: From H to Pu [J]. Computational Materials Science, 2014, 95: 337-50.

[13] MONKHORST H J, PACK J D. Special points for Brillouin-zone integrations [J]. Physical review B, 1976, 13(12): 5188.

[14] GRIMME S, ANTONY J, EHRLICH S, et al. A consistent and accurate ab initio parametrization of density functional dispersion correction (DFT-D) for the 94 elements H-Pu [J]. The Journal of chemical physics, 2010, 132(15): 154104.

[15] GRIMME S, EHRLICH S, GOERIGK L. Effect of the damping function in dispersion corrected density functional theory [J]. Journal of computational chemistry, 2011, 32(7): 1456-65.

[16] BAYLY C I, CIEPLAK P, CORNELL W D, et al. A Well-Behaved Electrostatic Potential Based Method Using Charge Restraints for Deriving Atomic Charges - the Resp Model [J]. J Phys Chem-Us, 1993, 97(40): 10269-80.

[17] LU T, CHEN F. Multiwfn: A multifunctional wavefunction analyzer [J]. Journal of computational chemistry, 2012, 33(5): 580-92.

[18] MOMMA K, IZUMI F. VESTA 3 for three-dimensional visualization of crystal, volumetric and morphology data [J]. J Appl Crystallogr, 2011, 44: 1272-6.

[19] HUMPHREY W, DALKE A, SCHULTEN K. VMD: Visual molecular dynamics [J]. J Mol Graph Model, 1996, 14(1): 33-8.